

Grain Size and Porosity Controlling of CeO₂ for Surrogate of UO₂ Fuel and Fracture Toughness Calculation

Jaejoon Kim^a, Qusai Mistarihi^a, Ho Jin Ryu^{a*}

^a Department of Nuclear and Quantum Engineering, KAIST, Yuseong-gu, Daejeon 34141, Republic of Korea

*corresponding author: hojinryu@kaist.ac.kr

1. Introduction

Uranium dioxide pellets, used as fuel for light water reactors, are subjected to extreme conditions during operation. High temperature, irradiation, and stress gradients have a significant effect on the microstructure of fuel pellets with a theoretical density of about 96% and a grain size of 7 μm before loading. High resonance neutron absorption of the fuel rim part locally increases the plutonium concentration, which results in higher fission density. The local burnup of the rim part of pellet is about two to three times higher than that of the center part, and due to the relatively low heat transfer coefficient of uranium dioxide, there is a large temperature difference between the center and the outside of the fuel. This difference in conditions creates a new structure called the high burnup structure outside the fuel.[1][2][3] Grain subdivisions are created, and existing micron-sized grains are transformed to less than 500 nm and produce parts with porosity of more than 20 %. The formation of this high burnup structure may act as another influential variable in the safety analysis of high burnup fuels and may affect fuel fragmentation in LOCA accidents. However, the strong radiotoxicity of real high burnup fuels requires expensive and complex safe handling to use it in real experiments. Therefore, ceramic materials with physical properties and crystal structure similar to those of actual nuclear fuel are used as analogous. Cerium oxide has been used as a surrogate material for uranium dioxide in many experiments because of the same crystal structure and similar thermal properties.[4] Experiments on the preparation of cerium oxide pellets using conventional powder metallurgy have already been reported.[5] Some experiments have been performed to examine the behavior of fission gas by implanting xenon or krypton in cerium oxide.[6][7] However, as mentioned above, the actual high burnup fuel has different porosity and grain size along the radial direction, and the existing experiments were conducted only with cerium oxide having about 5-10 μm and 5% porosity. The aim of this study was to prepare pellets by controlling the grain size and porosity of cerium oxide and to investigate the effect of these microstructure on the fragmentation behavior of high burnup fuel by measuring fracture toughness.

2. Methods

2.1 Grain size controlling of cerium oxide pellet

Samples were prepared by powder metallurgy. CeO₂ (Sigma aldrich, 99.9% <, ~5 μm) was used for sample preparation. To control grain size, it was manufactured in three different ways. The first specimen was pressed by uni-axial press at 100 MPa and then further pressed for 5 minutes at 300 MPa by cold isostatic press. After that, it was then sintered for 2 hours at 1500 °C in ambient air. As a second specimen, a ball milling technique was used to produce specimens with grain sizes of several hundred nanometers, such as the fuel rim part. 3 mm zirconia balls were used and powder was milled for 40 hours at 140 rpm in ethanol with a 1:20 ball powder ratio. After milling, powder was pressed by uni-axial press at 100 MPa and then further pressed for 5 minutes at 300 MPa by cold isostatic press and it was sintered at 1400 °C for 20 minutes using a microwave furnace in order to minimize grain growth by sintering. To obtain a large grain size sample for the third sample, dopant was added. Many experiments have been conducted with the addition of other oxide dopants to uranium dioxide and cerium oxide to control grain size. In this study, 0.3 at% of Fe₂O₃ was added to cerium oxide powder and then milled for 20 hours in a 1:2 powder ball ratio in ethanol using 2mm zirconia balls. Mixed powder was also pressed by uni-axial press at 100 MPa and then further pressed for 5 minutes at 300 MPa by cold isostatic press and sintered for 2 hours at 1500 °C in ambient air. The prepared specimens were thermally etched at 1300 °C for 10 minutes and then microstructure analysis was performed by Scanning electron microscope (SEM).

2.2 Porosity controlling of cerium oxide pellet

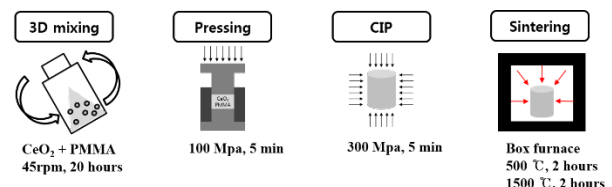


Figure 1. Simple schematic of fabrication of porosity controlled sample.

Poly(methyl methacrylate) (PMMA), about 3 μm in size, was used to produce artificial pores. This organic powder has a vaporization point of 200 °C, much lower than the sintering temperature of cerium oxide. PMMA powder in the green compact is vaporized at low temperature before sintering to form voids in the specimen. Figure 1 is a

Table 2. Powder metallurgy process: Experimental conditions.

Sample	Powder preparation	Pressing	Sintering method
Grain size control			
1	As received	100 MPa Uni-axial, 300 MPa CIP	1500 °C for 2 hours ambient air
2	Ball milled	100 MPa Uni-axial, 300 MPa CIP	1400 °C for 20 minutes in microwave furnace
3	0.03 at% Fe ₂ O ₃ doped	100 MPa Uni-axial, 300 MPa CIP	1500 °C for 2 hours ambient air
Porosity control			
1	As received	100 MPa Uni-axial, 300 MPa CIP	1500 °C for 2 hours ambient air
2	2.5 wt% PMMA mixed	100 MPa Uni-axial, 300 MPa CIP	1500 °C for 2 hours ambient air
3	5.0 wt% PMMA mixed	100 MPa Uni-axial, 300 MPa CIP	1500 °C for 2 hours ambient air

simplified depiction of a method for preparing specimens with controlled porosity. 0, 2.5 and 5 wt% of PMMA powder was added to cerium oxide, respectively, and mixed for 20 hours using a 3D mixer. Mixed powder was also pressed by uni-axial press at 100 MPa and then further pressed for 5 minutes at 300 MPa by cold isostatic press. After that, the PMMA is vaporized at 500 °C for 2 hours to form voids in the green compact, and then the temperature is raised again and sintered at 1500 °C for 2 hours. The density of the prepared specimens was measured and the microstructure was also examined by SEM. Table 1 shows a summary of the samples fabrication conditions by powder metallurgy process.

2.3 Hardness and fracture toughness measurement

It has long been recognized that indentation cracks can be related to the toughness of materials, and many papers have used them. [8][9][10][11]

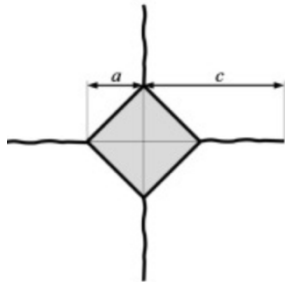


Figure 2. Simple illustration depicting indentation crack

$$K_C = 0.018 \left(\frac{E}{Hv} \right)^{0.5} \left(\frac{P}{c^{1.5}} \right) \quad (1)$$

Fracture toughness can be deduced with equation (1). K_C [MPa/ \sqrt{m}] is fracture toughness, Hv [GPa] is vicker's hardness of material, E [GPa] is Young's modulus of material, P [N] is indenting force to make crack, c [m] is length of crack from center of indentation mark described in Figure 2. In this case, Young's modulus is not constant because it is varying along the porosity of sample. Therefore, Young's modulus of samples corresponding each porosity was calculated also by Hanshin's theory. In this theory, pore is regarded as reinforcement which has zero modulus.

$$B = B_0 \left\{ 1 + \frac{3(v_0-1)p}{2(1-2v_0)+(1-v_0)p} \right\} \quad (2)$$

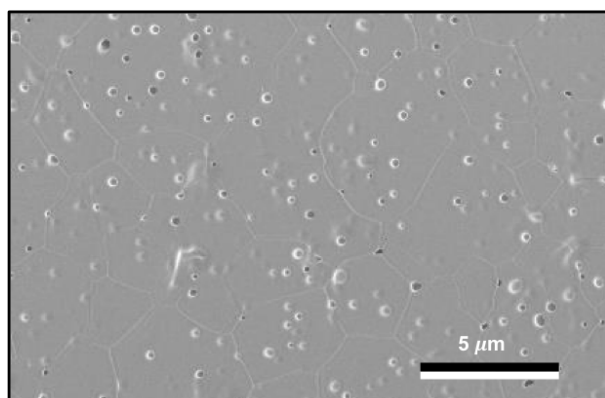
$$G = G_0 \left\{ 1 + \frac{15(v_0-1)p}{(7-5v_0)+2(4-5v_0)p} \right\} \quad (3)$$

$$E = \frac{3BG}{B+\frac{G}{3}} \quad (4)$$

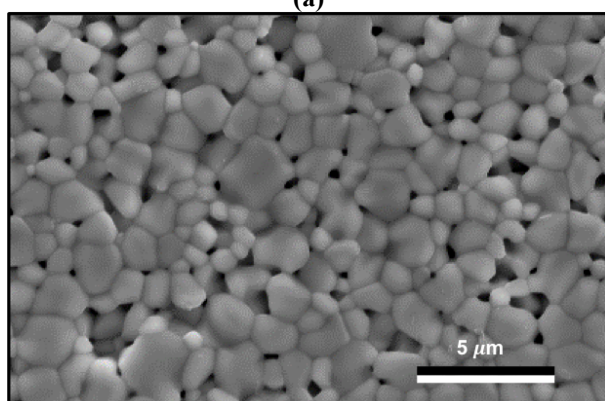
Bulk modulus, and shear modulus can be calculated by equation (2) and (3). According to Equation (4), Young's modulus can be derived from the combination of the two. In this equation, B_0 , G_0 , v_0 , are bulk modulus shear modulus and Poisson ratio of specimen without pore, respectively, and p is porosity.

3. Results and Discussion

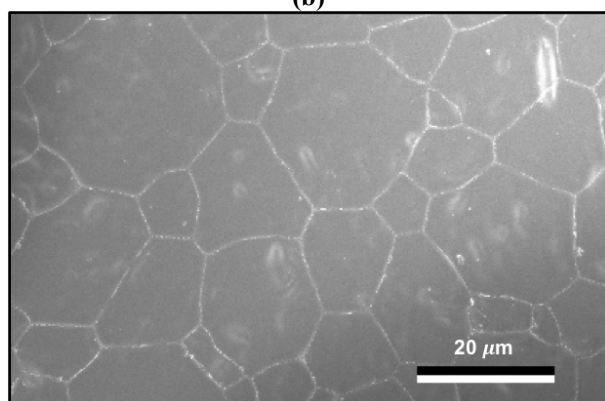
3.1 Grain size controlling of cerium oxide pellet



(a)



(b)



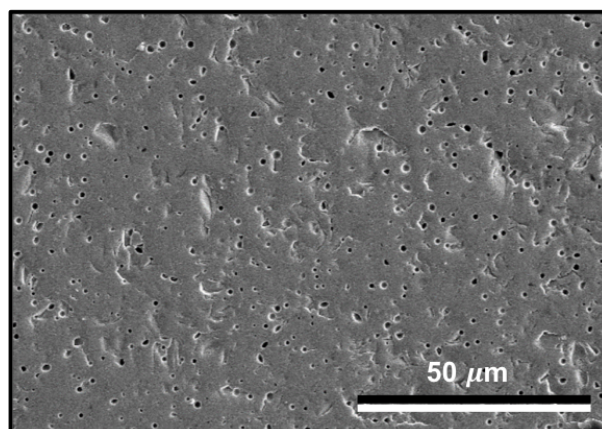
(c)

Figure 3. Microstructure of grain size controlled samples. (a) is medium size, (b) is small size, and (c) is large size.

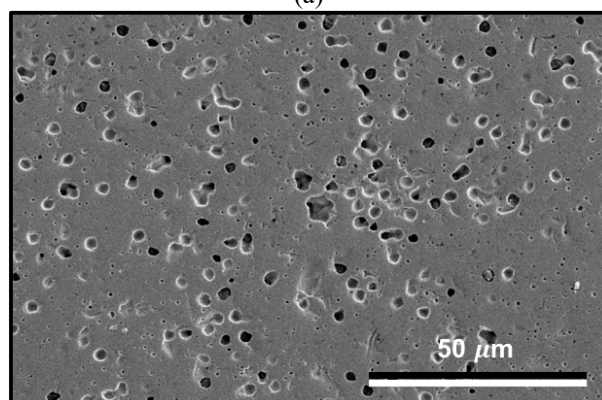
Figure 3 shows the SEM microstructure of grain size controlled samples after thermal etching. The middle size grain sample had an average of 6.8 μm, similar to the grain size of the actual uranium dioxide fuel before loading into the reactor, with a density of 96.9% of the theoretical density. Small size grain specimens made of milled powder had a grain size of about 0.6 micrometers, similar to the rim part of high burnup fuels, and had a theoretical density of 90.3%. The large size grain sample doped with Fe₂O₃ had a grain size of 20.0 μm on average and was full densified. When diffusivity was adjusted by sintering temperature, sintering method, and doping to control grain size, the changed variables influenced the densification. Therefore, specimens with larger grain

sizes tend to be denser.

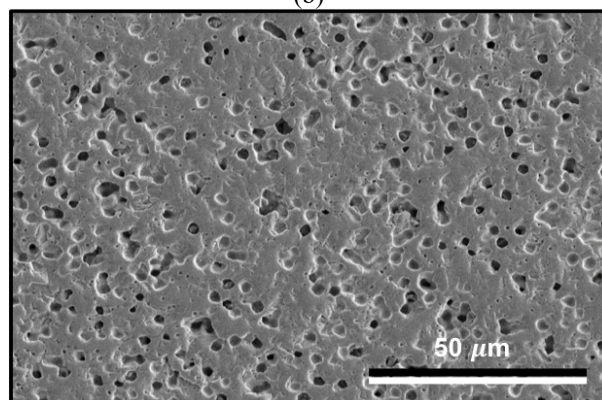
3.2 Porosity controlling of cerium oxide pellet



(a)



(b)



(c)

Figure 4. Microstructure of porosity controlled samples by PMMA addition. (a) 0 wt% PMMA, (b) 2.5 wt% PMMA, and (c) 5 wt% PMMA.

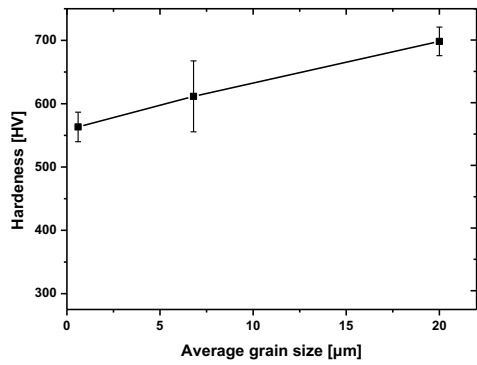
Figure 4 shows SEM images of porosity controlled samples. The density of each specimen was measured at 96.9%, 87.9%, and 80.6% of the theoretical density of cerium oxide, and samples with 5 wt% of PMMA had porosity similar to that of rim parts of high burnup fuel. Considering that the pore size is about 2 μm and that the existing PMMA powder size is 3 μm, the volumetric shrinkage of about 33% occurred during the sintering in

the remaining voids after the vaporization of PMMA.

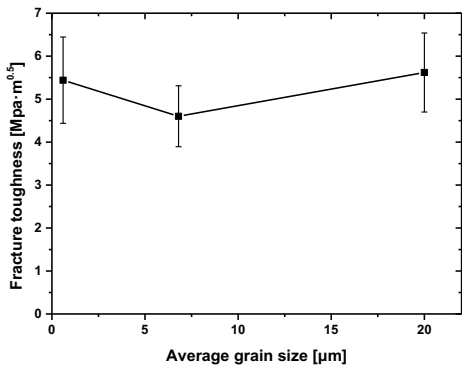
2.3 Hardness and fracture toughness measurement

Table 2. Bulk modulus, shear modulus, Young's modulus of grain size controlled samples.

Grain size [μm]	Density [%]	B [GPa]	G [GPa]	E[GPa]
0.6	90.3	161	81	209
6.8	96.9	188	90	234
20.0	100	204	96	249



(a)



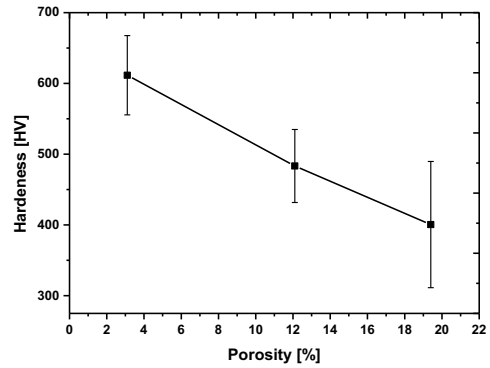
(b)

Figure 5. (a) Hardness and (b) fracture toughness of grain size controlled samples.

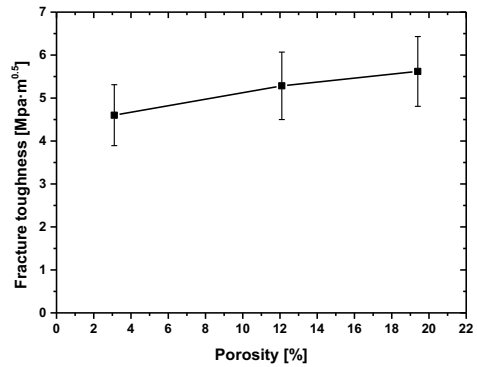
The bulk modulus, shear modulus, and Young's modulus calculated by equations (2), (3) and (4) are summarized in Table 2. Figure 5 shows (a) the hardness values of the grain size controlled specimens and (b) the fracture toughness values calculated using equation (1). Contrary to the results of other experiments, the larger the grain size, the higher the hardness. The above results were obtained because the effect of porosity on hardness was greater than the effect of grain size on hardness. The fracture toughness values influenced by the elastic modulus and hardness did not show much tendency for these specimens.

Table 3. Bulk modulus, shear modulus, Young's modulus of porosity controlled samples.

Density [%]	B [GPa]	G [GPa]	E[GPa]
96.9	188	91	234
87.9	146	76	194
80.6	116	66	166



(a)



(b)

Figure 6. (a) Hardness and (b) fracture toughness of porosity controlled samples.

The bulk modulus, shear modulus, and Young's modulus of the porosity controlled sample are described in Table 3. As shown in Figure 6 (a), the hardness values of the porosity controlled sample decreased significantly as the porosity increased. As shown in Figure 6 (b), the fracture toughness did not change significantly with the porosity, considering the size of the error bar. The pores in the specimen serve as both an obstacle to crack propagation and an open space for the crack to begin. The interaction of these complex factors did not significantly affect the fracture toughness. In summary, the hardness value was more affected by the porosity than the grain size of the specimen, and it was difficult to say that the fracture toughness showed a significant change. It can be concluded that the difference in fracture toughness between the rim part and the core of the actual high burnup fuel caused by the microstructure difference can

be neglected.

4. Conclusion

Current research was mainly performed by controlling the grain size and porosity of cerium oxide for the simulation of high burnup fuel and measuring the hardness and fracture toughness of the prepared samples. Grain size was controlled by milling, Fe₂O₃ doping, sintering temperature and sintering method. Porosity was controlled by vaporizing PMMA powder before sintering. Microstructure analysis and density measurement of the prepared specimens were performed also. The hardness of these specimens was measured and the fracture toughness calculated by measuring the hardness and crack length was also derived.

REFERENCES

[1] P. Rudling, R. Adamson, B. Cox, F. Garzarolli, A. Strasser, High burnup fuel issues, *Nucl. Eng. Technol.* 40 (2008) 1–8. doi:10.5516/NET.2008.40.1.001.

[2] V. V. Rondinella, T. Wiss, The high burn-up structure in nuclear fuel, *Mater. Today*. 13 (2010) 24–32. doi:10.1016/S1369-7021(10)70221-2.

[3] Y.H. Koo, B.H. Lee, J.Y. Oh, D.S. Sohn, The width of high burnup structure in LWR UO₂ fuel, in: *Am. Nucl. Soc. - 2007 LWR Fuel Performance/Top Fuel*, 2007: pp. 317–324.

[4] H.S. Kim, C.Y. Joung, B.H. Lee, J.Y. Oh, Y.H. Koo, P. Heimgartner, Applicability of CeO₂ as a surrogate for PuO₂ in a MOX fuel development, *J. Nucl. Mater.* 378 (2008) 98–104. doi:10.1016/j.jnucmat.2008.05.003.

[5] C. García-Ostos, J.A. Rodríguez-Ortiz, C. Arévalo, J. Cobos, F.J. Gotor, Y. Torres, Fabrication and characterization of CeO₂ pellets for simulation of nuclear fuel, *Nucl. Eng. Des.* 298 (2016) 160–167. doi:10.1016/j.nucengdes.2015.12.026.

[6] B. Ye, A. Oaks, M. Kirk, D. Yun, W.Y. Chen, B. Holtzman, J.F. Stubbins, Irradiation effects in UO₂ and CeO₂, *J. Nucl. Mater.* 441 (2013) 525–529. doi:10.1016/j.jnucmat.2012.09.035.

[7] W.J. Weber, ALPHA-IRRADIATION DAMAGE IN CeO₂, UO₂ AND PuO₂., *Radiat. Eff.* 83 (1984) 145–156. doi:10.1080/00337578408215798.

[8] J. Akbaridoost, Size and crack length effects on fracture toughness of polycrystalline graphite, *Eng. Solid Mech.* 2 (2014) 183–192. doi:10.5267/j.esm.2014.4.005.

[9] P. CHANTIKUL, G.R. ANSTIS, B.R. LAWN, D.B. MARSHALL, A Critical Evaluation of Indentation Techniques for Measuring Fracture Toughness: II, Strength Method, *J. Am. Ceram. Soc.* 64 (1981) 539–543. doi:10.1111/j.1151-2916.1981.tb10321.x.

[10] C.B. Ponton, R.D. Rawlings, Vickers indentation fracture toughness test Part 1 review of literature and formulation of standardised indentation toughness equations, *Mater. Sci. Technol. (United Kingdom)*. 5 (1989) 865–872. doi:10.1179/mst.1989.5.9.865.

[11] C.B. Ponton, R.D. Rawlings, Vickers indentation fracture toughness test Part 2 application and critical evaluation of standardised indentation toughness equations, *Mater. Sci. Technol. (United Kingdom)*. 5 (1989) 961–976. doi:10.1179/mst.1989.5.10.961.